J Appl Electrochem (2009) 39:339–345
DOI 10.1007/s10800-008-9677-1

ORIGINAL PAPER

Corrosion behavior of composition modulated multilayer Zn–Co electrodeposits produced using a single-bath technique

V. Thangaraj · N. Eliaz · A. Chitharanjan Hegde

Received: 10 October 2007 / Accepted: 1 October 2008 / Published online: 21 October 2008

Abstract Composition modulated alloy (CMA) electrodeposits of Zn–Co were produced from acid chloride baths by the single-bath technique. Their corrosion behavior was evaluated as a function of the switched cathode current densities and the number of layers. The process was optimized with respect to the highest corrosion resistance. Enhanced corrosion resistance was obtained when the outer layer was slightly richer with cobalt. At the optimum switched current densities 40/55 mA cm^{-2}, a coating with 600 layers showed $\sim$6 times higher corrosion resistance than monolithic Zn–Co electrodeposit having the same thickness. The CMA coating exhibited red rust only after 1,130 h in a salt-spray test. The increased corrosion resistance of the multilayer alloys was related to their inherent barrier properties, as revealed by Electrochemical Impedance Spectroscopy. The corrosion resistance was explained in terms of *n*-type semiconductor films at the interface as supported by Mott–Schottky plots.

Keywords Electrodeposition · Composition modulated alloy (CMA) · Anomalous codeposition · Zn–Co coatings · Corrosion resistance

V. Thangaraj · A. C. Hegde (✉)
Department of Chemistry, National Institute of Technology Karnataka, Surathkal, Srinivasnagar 575 025, India
e-mail: achegde@rediffmail.com

N. Eliaz
Biomaterials and Corrosion Laboratory, Tel-Aviv University, Ramat-Aviv 69978, Israel

1 Introduction

Codeposition of two metals requires that their individual reversible potentials are reasonably close to each other in the specific bath. This is the case when their standard potentials are close, when the concentration of one of the metals in solution is properly tuned, or when a complexing agent that forms complexes with different stability constants is added [1].

Eliaz and Gileadi [1] have recently reviewed the principles of alloy deposition and the phenomenon of anomalous codeposition (ACD) in the framework of a more comprehensive review of induced codeposition. The term anomalous codeposition was coined by Brenner [2] to describe an electrochemical deposition process in which the less noble metal is deposited preferentially under most plating conditions. This behavior is typically observed in codeposition of iron-group metals (i.e. Fe, Co and Ni), or in codeposition of an iron-group metal with Zn or Cd, with either inhibition or acceleration of the rate of deposition of one of the alloying elements by the other [1, 2]. Even if the concentrations of two metal ions in the plating bath are equal, their concentrations at the surface, which determine the rate of deposition, may be quite different, if their partial current densities are different. During alloy plating, the deposition of the two metals may be under different degrees of mass-transport limitation. Thus, alloy coatings of graded or alternating composition can be produced in the same solution by changing the applied current density [1].

Electrodeposition of composition modulated alloys (CMA's) has found much interest in recent years because such alloys possess improved corrosion, mechanical, magnetic and electrical properties [2–18]. These properties can be tuned by several factors, including the layer thickness, the overall thickness, the chemical composition of

each individual layer, and the periodicity of layers. There are two major ways to produce CMA electrodeposits. The dual bath technique (DBT) [14] involves the deposition of constituents from two separate plating baths in an alternate manner. Any combination of layers can be formed, provided that each can be individually deposited, and very thin metal or alloy films can easily be formed. However, DBT has some significant drawbacks. First, it might be difficult to achieve the appropriate structure because of the periodic exposure of the substrate to potential contaminants during the transfer from one bath to another. In addition, the process might be more time consuming and difficult to automate in comparison to the alternative technique. In the single bath technique (SBT) [4, 7, 9], the metal ions required to form both deposit layers are contained in a single electrolyte, and alloy deposition is achieved by alternately changing the plating current/potential, possibly in combination with a modulation of the mass transport toward the cathode. Although substantial success has been achieved with the SBT, the selection of constituents is limited because their deposition potentials must be sufficiently different to allow a separate electrodeposition of each. Difficulties can also be encountered in the deposition of very thin layers due to the relaxation time for the redistribution of solutes in the diffusion double layer.

Kalantary et al. [19] obtained Zn–Ni CMA coatings with an overall thickness of 8 μm. Chawa et al. [17] showed that Zn–Ni CMA coatings had better corrosion resistance than that of monolithic Zn–Ni coatings of similar thickness. Liao et al. [20–22] applied both the SBT and the DBT for deposition of Zn/Zn–Fe and Zn–Fe coatings. Kirilova et al. [23–25] obtained CMA coatings of Zn–Co by means of both the SBT and the DBT. The coatings obtained from a single bath dissolved at more positive potentials, as compared with pure Zn coatings, but much more negative than the dissolution potentials of pure Co coatings. As the number of layers was increased, regardless of their thickness and sequence, the dissolution potentials were shifted in the positive direction. The corrosion potentials of the CMA's deposited from a single bath were significantly more positive than those deposited from a dual bath. The best corrosion resistance was found for multilayers consisting of four sublayers, each 3.0 μm thick. No red rust appeared on the surface of CMA's with an outer layer of Zn, Co or Zn–1%Co even after 1,584 h in a salt spray corrosion test. The iridescent yellow chromating of CMA's consisting of a high number of thin layers deteriorated their corrosion resistance.

Although the improvement in the corrosion resistance of Zn–Co CMA electrodeposits has been widely reported, very little has been done with respect to optimization of the deposition conditions in a SBT so as to obtain the best corrosion resistance. Recently, two of us have optimized a chloride bath for production of CMA Zn–Ni coatings over mild steel (V.T. and A.C.H., J. Mater. Sci., communicated). These coatings were found to have ~50 times higher corrosion resistance than conventional Zn–Ni coatings of the same thickness. Being inspired by the results of that work, the objective of the present work was to optimize the CMA Zn–Co electrodeposits with respect to corrosion resistance.

2 Experimental details

Monolithic Zn–Co alloys were formed at current densities of either 40 or 50 mA cm^{-2} from an optimized bath containing 80 mg cm^{-3} $ZnCl_2$, 7 mg cm^{-3} $CoCl_2$, 75 mg cm^{-3} NH_4Cl, 70 mg cm^{-3} KCl, 7 mg cm^{-3} glycine and 10 mg cm^{-3} gelatin. The SBT was applied. The electrolyte contained Zn^{2+} and Co^{2+} ions and was prepared using LR-grade chemicals and distilled water. A precleaned mild steel sample (2 × 2 cm) was used as a cathode, and pure zinc as an anode. Depositions were carried out galvanostatically in a constantly stirred electrolyte maintained at pH = 4 and $T = 30$ °C. All depositions and subsequent electrochemical characterizations were conducted using a Metrohm PGSTAT 30.

The periodic change of current density allowed the growth of layers with alternating chemical compositions. Pulses of low current density resulted in layers with low Co concentration, whereas pulses of high current density resulted in layers with higher Co concentration. These two types of layers will be termed hereafter $(Zn–Co)_1$ and $(Zn–Co)_2$, respectively. The sequence $(Zn–Co)_1/(Zn–Co)_2$ shall represent configuration in which the first layer, on top of the steel substrate, has low Co content whereas the outer, top layer has higher Co content. By reversing the order of the switched current densities, the opposite configuration, marked hereafter as $(Zn–Co)_2/(Zn–Co)_1$, was obtained. The thickness of each layer was controlled by the width (duration) of each current pulse. In addition, the total number of layers was controlled by the number of repeating cycles. The corrosion studies were made at 25 °C in aerated 5% NaCl solution at pH = 6, prepared in distilled water. The polarization curves were obtained by cathodic and anodic potentiodynamic polarizations at a scan rate of 1 mV s^{-1}. The reference electrode was saturated calomel electrode (SCE), while platinum electrode was the counter electrode. The impedance behavior of Zn–Co alloy deposits was studied by drawing the Nyquist plot in the frequency range from 100 kHz to 5 mHz. The composition of the coatings was determined colorimetrically by a standard method (involving stripping of the deposit in dilute HCl). The microstructure of CMA deposits was examined by scanning electron microscopy (SEM, model

JSM-6380 LA from JEOL, Japan). The associated Energy Dispersive X-ray Analysis (EDXA) allowed for composition estimation. The thicknesses of the deposits were calculated using Faraday's law.

3 Results and discussion

3.1 Monolithic Zn–Co coating

Using the optimized bath composition given in the previous section, bright and smooth monolithic Zn–Co coatings were produced on mild steel. The deposit produced at 40 mA cm^{-2} contained 0.51 wt.% Co and exhibited corrosion rate of 888.6 μm y^{-1}. The deposit produced at 50 mA cm^{-2} contained 0.57 wt.% Co and exhibited corrosion rate of 476.3 μm y^{-1} (see Table 1). CMA Zn–Co coatings were produced with different number/sequence of sublayers while keeping the same overall thickness (~15 μm), and their corrosion rate was measured.

3.2 Zn–Co CMA coatings

3.2.1 Optimization of the switched cathode current densities

It is well known that, in the case of alloys of zinc with iron-group metals, even a small change in the concentration of the latter may result in significant properties change due to change in the phase structure. Thus, precise control of the switched current densities allowed production of alternate layers with different compositions and, consequently, different properties.

Table 1 The corrosion potential (E_{corr}), corrosion current density (i_{corr}) and corrosion rate (*CR*) of monolithic and CMA Zn–Co coatings

i_c (mA cm^{-2})	E_{corr} (V vs. SCE)	i_{corr} (μA cm^{-2})	CR (μm y^{-1})
Monolithic Zn–Co coatings			
40	−1.226	62.03	888.6
50	−1.168	33.25	476.3
CMA Zn–Co coatings, 10 mA cm^{-2} difference, 20 sublayers			
20/30	−1.092	17.48	258.1
30/40	−1.116	12.14	179.4
40/50	−1.171	9.475	139.9
50/60	−1.160	11.2	165.4
CMA Zn–Co coatings, 15 mA cm^{-2} difference, 20 sublayers			
20/35	−1.100	11.56	170.8
30/45	−1.142	9.627	142.2
40/55	−1.285	7.621	112.6
50/65	−1.168	10.28	151.8

The effect of different combinations of switched current densities on the corrosion behavior of the CMA coatings is demonstrated. Total deposition time: 10 min

Table 1 demonstrates the effect of the switched cathode current densities on the corrosion behavior. The lowest corrosion rate was measured in the case of $(Zn–Co)_1/(Zn–Co)_2$ coatings produced at 40/55 mA cm^{-2}. These coatings were also bright and uniform. This combination of current densities was selected for further study of the effects of the number of layers and the sequence of current densities, as described in the following subsection and in Table 2.

3.2.2 Optimization of the overall number of layers

The properties of CMA electrodeposits, including their corrosion resistance, may often be improved by increasing the total number of layers (usually, up to an optimal number), as long as the adhesion between layers is not deteriorated. Therefore, at the optimal combination of current densities identified before (40/55 mA cm^{-2}), CMA coatings with 20, 30, 60, 120, 300 and 600 sublayers (the latter, for example, reflects 300 layers from each composition) were produced. As evident from Table 2, the corrosion rate decreased substantially as the overall number of layers was increased, regardless of whether the configuration was $(Zn–Co)_1/(Zn–Co)_2$ or $(Zn–Co)_2/(Zn–Co)_1$. The lowest corrosion rate (83.8 μm y^{-1}) was obtained for a coating with the $(Zn–Co)_1/(Zn–Co)_2$ configuration and 600 sublayers. It is likely that further increase of the number of layers would result in further improvement of the corrosion resistance. In Table 2 it should also be noted that, for the same number of layers, the corrosion rate of the $(Zn–Co)_2/(Zn–Co)_1$ configuration is always higher than that of the $(Zn–Co)_1/(Zn–Co)_2$ configuration. This implies that the presence of a top, outer layer only slightly richer with Co in the latter configuration is indeed beneficial with respect to corrosion resistance.

Figure 1 shows the potentiodynamic polarization curves related to the CMA coatings with the $(Zn–Co)_1/(Zn–Co)_2$ configuration but with different number of layers. Tafel extrapolation on such curves resulted in determination of the corrosion potential, corrosion current density and corrosion rate, as listed in Table 2. The first peak within the anodic regime corresponds to the selective dissolution of Zn. As mentioned before, the increase of the number of layers resulted in a decrease in the corrosion rate (or, a decrease in the corrosion current density).

3.3 Comparison between the corrosion behavior of monolithic and CMA Zn–Co coatings

Comparing the values given in Tables 1 and 2, it becomes apparent that the corrosion rate of the CMA coating with

Table 2 The effect of the overall number of layers and their sequence on the corrosion potential, corrosion current density and corrosion rate of CMA Zn–Co coatings electrodeposited at the optimal combination of current densities (40/55 mA cm^{-2})

Configuration	Number of sublayers	E_{corr} (V vs. SCE)	i_{corr} (μA cm^{-2})	CR (μm y^{-1})
$(Zn–Co)_1/(Zn–Co)_2$, (40/55 mA cm^{-2})	20	−1.285	7.621	112.6
	30	−1.289	7.60	108.7
	60	−1.239	7.141	105.5
	120	−1.226	6.67	98.3
	300	−1.246	6.17	91.1
	600	−1.267	5.673	83.8
$(Zn–Co)_2/(Zn–Co)_1$, (55/40 mA cm^{-2})	20	−1.120	10.18	150.3
	30	−1.124	9.228	136.3
	60	−1.138	8.24	121.7
	120	−1.150	8.10	119.7
	300	−1.174	6.55	96.7
	600	−1.222	7.402	109.2

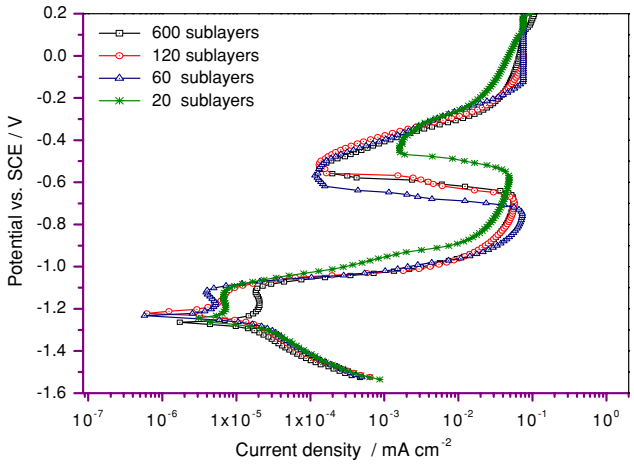

Fig. 1 Potentiodynamic polarization curves of CMA $(Zn–Co)_1/(Zn–Co)_2$ coatings with varying overall number of layers. Scan rate: 1.0 mV s^{-1}

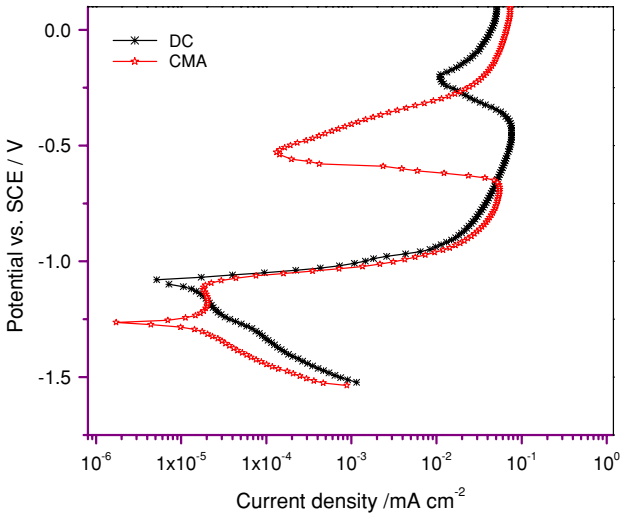

Fig. 2 Potentiodynamic polarization curves of monolithic and $(Zn–Co)_1/(Zn–Co)_2$ CMA Zn–Co coatings of the same thickness

the $(Zn–Co)_1/(Zn–Co)_2$ configuration and 600 sublayers is 5.7–10.6 times lower than that of the monolithic Zn–Co coating with the same thickness. Thus, it may be concluded that the CMA coating, when designed properly, provides significant improvement in the protection of steel against corrosion.

Electrochemical Impedance Spectroscopy (EIS) is a useful technique for ranking coatings, assessing interfacial reactions, quantifying coating breakdown, and predicting the lifetime of coating/metal systems. It has been used, for example, to monitor the underfilm corrosion of polymer-coated cobalt [26, 27]. Advantages of this technique over dc techniques include the absence of any significant perturbation to the system, its applicability to the assessment of low-conductivity media, and the existence of a frequency component that may provide mechanistic information. Figures 2 and 3 demonstrate the difference between the monolithic and the CMA coatings in terms of the potentiodynamic polarization curve and Nyquist plot, respectively.

The formation of a passive layer only on the CMA coating is evident in Fig. 2. The Nyquist plots in Fig. 3 indicate on a possible change in the electronic structure of the CMA coating, compared to the monolithic coating. The solution resistance R_s is nearly identical in both cases as the same bath chemistry and cell configuration were used. The significantly higher impedance of the CMA coating reflects its higher corrosion resistance. An inductive loop is evident at low frequencies. The larger diameter of the (unfinished) semicircle in the case of the CMA coating reflects increased corrosion resistance, which is attributed to a change in the film (coating) capacitance C_f. The capacitive impedance at high frequencies is well related to the thickness and the dielectric constant of the film. No diffusion-limited process, in the form of Warburg impedance, is evident.

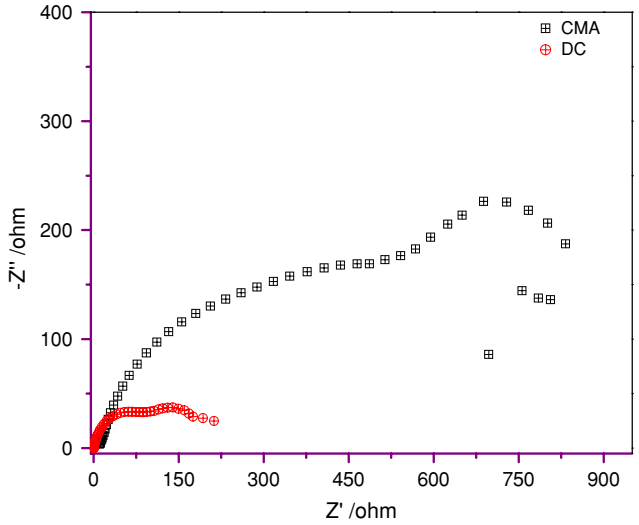

Fig. 3 Nyquist EIS plots for monolithic and $(Zn–Co)_1/(Zn–Co)_2$ CMA coatings of the same thickness

Figure 4 compares the corrosion rates of monolithic Zn, monolithic Zn–Co, CMA Zn–Ni, CMA $(Zn–Co)_1/(Zn–Co)_2$ and CMA $(Zn–Co)_2/(Zn–Co)_1$ coatings having the same overall thickness. It is apparent that while the CMA $(Zn–Co)_1/(Zn–Co)_2$ coating provides the higher corrosion resistance compared to all other Zn–Co (and pure Zn) coatings, $(Zn–Ni)_1/(Zn–Ni)_2$ provides even higher corrosion resistance. Complementary neutral salt spray tests were conducted, and the corrosion resistance was evaluated also in terms of the time to the appearance of red rust on the surface. All CMA Zn–Co coatings demonstrated longer times to red rust than the monolithic Zn–Co coating with similar thickness (1,130 vs. 600 h, respectively).

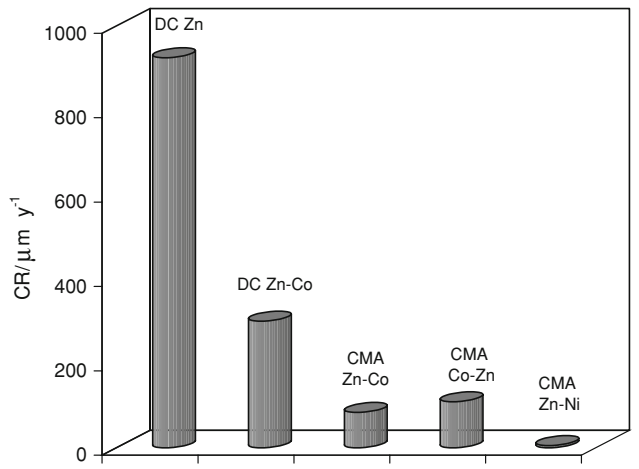

Fig. 4 Comparison between the corrosion rates of three CMA and two monolithic (DC) coatings with the same thickness. CMA Zn–Co represents the $(Zn–Co)_1/(Zn–Co)_2$ configuration, whereas CMA Co–Zn represents the $(Zn–Co)_2/(Zn–Co)_1$ configuration

3.4 SEM/EDXA characterization of the CMA coatings

The formation of alternate layers of $(Zn–Co)_1$ and $(Zn–Co)_2$, deposited at two different cathode current densities, was confirmed by scanning electron microscopy (SEM). A view of the cross-section of a coating consisting of 20 layers, which was deposited at the optimized 40/55 mA cm^{-2} combination, is shown in Fig. 5a. The poor contrast may be ascribed to almost similar chemical composition of each sublayer. EDXA analysis showed that the $(Zn–Co)_1$ layer contained approximately 0.57 wt.% Co, while the $(Zn–Co)_2$ layer contained approximately 0.64 wt.% Co. Figure 5b shows the surface morphology of the same deposit, with deposition time of 30 s per layer. It was observed that the surface homogeneity deteriorated as the thickness of the layer was increased, possibly due to mass transport limitations and/or occurrence of local electrocrystallization events within the layer.

3.5 The mechanism of corrosion protection by the CMA Zn–Co coatings

Figure 6 shows the Nyquist plots of CMA Zn–Co coatings with $(Zn–Co)_1/(Zn–Co)_2$ configuration but with a different overall number of layers. As the number of layers is increased, the impedance of the coating increases too, thus representing improved corrosion resistance. It is well known that the corrosion product film on most alloys exhibit semiconductive behavior [28, 29]. The most common in situ method for probing the electronic properties of the corrosion product film is the Mott–Schottky analysis. The linear relation between $1/C^2$, where C is the interfacial capacitance, and the applied potential E is expressed as Mott–Schottky equation:

$$\frac{1}{C^2} = \frac{2}{\varepsilon\,\varepsilon_0\,e\,N}\left(E - E_{\mathrm{fb}} - \frac{kT}{e}\right) \tag{1}$$

where ε is the dielectric constant of the film, ε_0 the vacuum permittivity, e the electron charge, N the acceptor concentration in the product film, k Boltzmann constant, T the absolute temperature, and E_{fb} the flat band potential. The type of semiconductor can be determined from the $1/C^2$ versus E plot. A negative slope indicates a p-type semiconductor, whereas a positive slope indicates an n-type semiconductor.

Figure 7 shows the C^{-2} versus E profile for a CMA Zn–Co coating with $(Zn–Co)_1/(Zn–Co)_2$ configuration, deposited at the optimized processing parameters. The positive slope of graph indicates that the protective layer is acting like an n-type semiconductor. For comparison, Hong et al. [30] explained the corrosion behavior of pure Ti versus Ti–Ag alloy in terms of an n-type

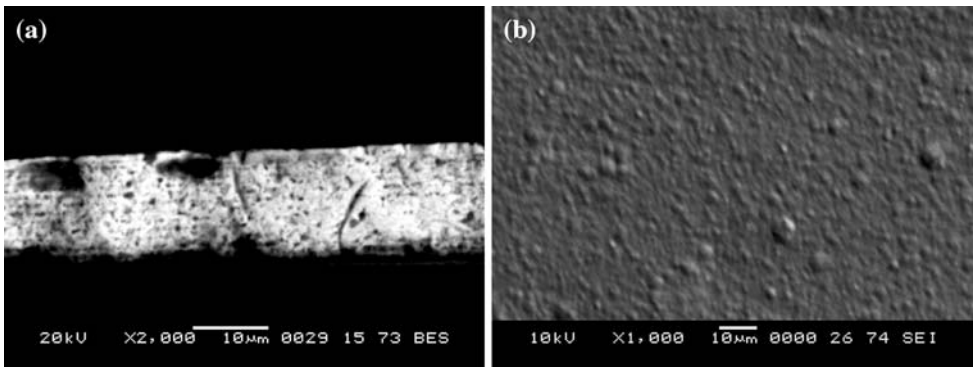

Fig. 5 SEM images of the cross-section (**a**) and top surface (**b**) of a CMA Zn–Co coating consisted of 20 sublayers

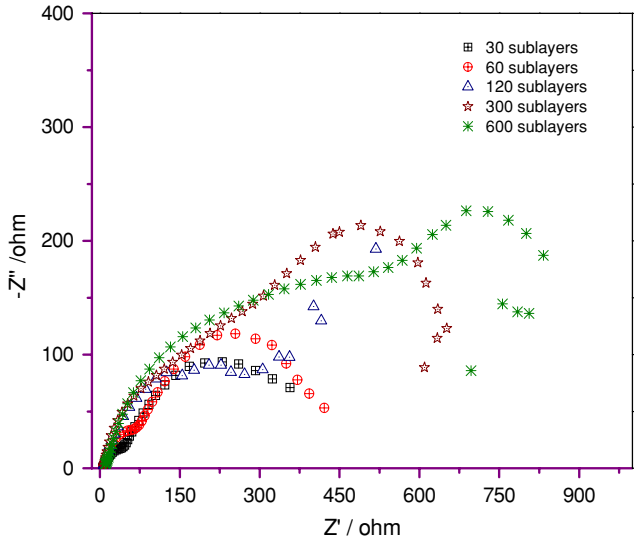

Fig. 6 Nyquist plots of CMA Zn–Co coatings with $(Zn–Co)_1/(Zn–Co)_2$ configuration but different numbers of layers

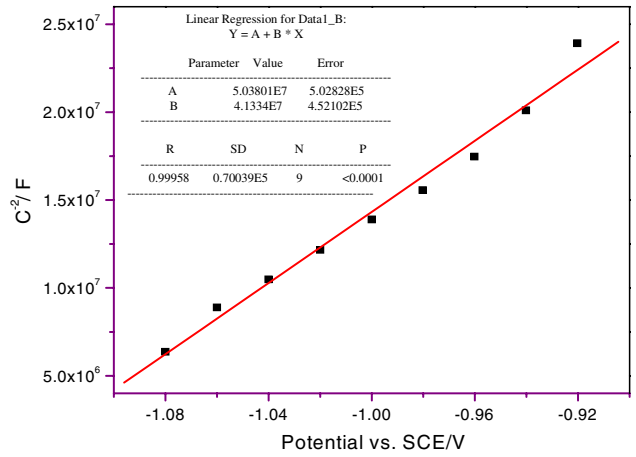

Fig. 7 Mott–Schottky plot for a CMA Zn–Co coating with $(Zn–Co)_1/(Zn–Co)_2$ configuration at the optimized processing parameters

semiconductor containing oxygen vacancies, the migration of which controls the kinetics of corrosion in neutral solutions.

4 Conclusions

The corrosion resistance of CMA Zn–Co electrodeposits was shown to be higher than that of the monolithic Zn–Co coating with the same thickness. For example, the corrosion rate of the CMA coating with the $(Zn–Co)_1/(Zn–Co)_2$ configuration and 600 sublayers was 5.7–10.6 times lower than that of the monolithic Zn–Co coating with the same thickness. The corrosion rate of the CMA coating decreased as the number of layers was increased, and as the sequence of switched current densities was determined so that the outer, top layer of the coating had higher concentration of cobalt. Even a small change in the content of cobalt in the layer was sufficient to change the corrosion resistance significantly. The electrochemical stability of the optimized CMA coating was explained in terms of an *n*-type semiconductor. It was demonstrated that optimization of the corrosion resistance is possible through proper manipulation of the deposition conditions and the structure of the coating.

Acknowledgment Thangaraj V. is grateful to NITK, Surathkal, for providing the Institute Fellowship that allowed carrying out this work.

References

1. Eliaz N, Gileadi E (2008) In: Vayenas CG, White RE, Gamboa-Aldeco ME (eds) Modern aspects of electrochemistry, vol 42. Springer, New York, pp 191–301
2. Brenner A (1963) Electrodeposition of alloys, vol II. Academic Press, New York
3. Blum W (1921) Trans Am Electrochem Soc 40:307
4. Cohen U, Koch FB, Sard R (1983) J Electrochem Soc 130:1987
5. Swathirajan S (1986) J Electrochem Soc 133:671
6. Ogden C (1986) Plat Surf Finish 5:133
7. Yahalom J, Zadok O (1987) J Mater Sci 22:499
8. Despić AR, Jović VD (1987) J Electrochem Soc 134:3004
9. Lashmore DS, Dariel MP (1988) J Electrochem Soc 135:1218
10. Despić AR, Jović VD, Spaić S (1989) J Electrochem Soc 136:1651
11. Barral G, Maximovitch S (1990) J Phys Colloques 51:C4-291
12. Wilcox GD, Gabe DR (1993) Corros Sci 35:1251
13. Kalantary MR (1994) Plat Surf Finish 81:80

14. Haseeb ASM, Celis JP, Roos JR (1994) J Electrochem Soc 141:230
15. Ross CA (1994) Annu Rev Mater Sci 24:159
16. Gabe DR, Green WA (1998) Surf Coat Technol 105:195
17. Chawa G, Wilcox GD, Gabe DR (1998) Trans Inst Metal Finish 76:117
18. Nabiyouni G, Schwarzacher W, Rolik Z, Bakonyi I (2002) J Magn Magn Mater 253:77
19. Kalantary MR, Wilcox GD, Gabe DR (1998) Br Corros J 33:197
20. Liao Y, Gabe DR, Wilcox GD (1998) Plat Surf Finish 85:60
21. Liao Y, Gabe DR, Wilcox GD (1998) Plat Surf Finish 85:62
22. Liao Y, Gabe DR, Wilcox GD (1998) Plat Surf Finish 85:88
23. Kirilova I, Ivanov I, Rashkov (1998) J Appl Electrochem 28:637
24. Kirilova I, Ivanov I, Rashkov (1998) J Appl Electrochem 28:1359
25. Kirilova I, Ivanov I (1999) J Appl Electrochem 29:1133
26. Cantini NJ, Mitton DB, Eliaz N, Leisk G, Wallace SL, Bellucci F, Thompson GE, Latanision RM (2000) Electrochem Solid State Lett 3:275
27. Mitton DB, Wallace SL, Cantini NJ, Bellucci F, Thompson GE, Eliaz N, Latanision RM (2002) J Electrochem Soc 149:B265
28. Stimming U (1986) Electrochim Acta 31:415
29. Sikora E, Macdonald D (2002) Electrochim Acta 48:69
30. Hong SB, Eliaz N, Sachs EM, Allen SM, Latanision RM (2001) Corr Sci 43:1781